

Determination of Cross Section for Different Fusion Reactions in Terms of Lattice Effects in Solid State Internal Conversion in Crystalline Palladium Environment

Abstract

In the article, we determine the cross section for different fusion reactions : $D(d,p)T$, $D(d,\gamma)^4\text{He}$, $T(d,n)^4\text{He}$ and $D(p,\gamma)^3\text{He}$ considering the lattice effect in internal conversion of solid state in palladium environment which is a metal with face cubic-centered structure. Fusionable particles are solved as sublattice, these particles contribute in fusion reaction in palladium environment. Fusion reaction is generated by flux of incoming fusionable particles. Bloch function for the initial and final state of three- body system from this fusion cross section can be estimated for above reactions. Thus lattice effect is calculated for mentioned reactions. Three- body system consists of the host lattice, sublattice and incident particles. Then it is compared with those of an ordinary fusion reaction. Finally, the internal conversion coefficient is obtained with regarding the lattice effect. The authors strongly discuss that the lattice effect in solid state internal conversion must be considered until the experimental data of fusion cross section have a good justification with theoretical hypothesis.

Key words: palladium, fusion, crystals, cross section

1. Introduction

Nowadays using nuclear energy is very important as a clean source of energy. There are two kinds of nuclear reactions, fusion and fission. Since fusion reaction has less radioactive radiation and the fusion fuels required for these reactions are more sufficiently available in the nature, therefore fusion reactions are important to study.

The ability of palladium to absorb hydrogen was recognized as early as the nineteenth century by Thomas Graham [1]. In 1989, observations of Stanley Pons and Martin Fleischmann about fusion in room temperature gained a lot of attention [2]. After that, the word “**cold fusion**” was used for Low-Energy Nuclear Reactions (**LENR**) [3]. From 1989 to 1992, all hypotheses about cold fusion failed [3]. In 1995, many years after Pons and Fleischmann’s separation, Fleischmann continued his researches and published many articles [4]. Although many groups had studied this subject, cold fusion was not accepted officially. The cross section of fusion reactions in metallic environments indicated significant enhancement and its reason have not been proved yet [5]. Meanwhile, one of the controversial hypotheses was electron screening for host particles [3]. In 2007, after many researches, finally cold fusion was accepted officially. Now one of the most controversial issues is cold fusion in metallic crystalline environments [6].

In 2002, Peter Kalman and Thomas Keszthelyi studied this problem on different metals. They investigated many different factors to explain the enhancement of fusion cross section. For example, the electron screening was checked for 29 deuterated metals and 5 deuterated insulators/semiconductors from Periodic Tables. Among them, metals were most convenient. A

few factors that are investigated on fusion cross section are: stopping power, thermal motion, channeling, diffusion, conductivity, and crystal structure and electron configuration. None of them could explain and analyses the observed enhancement crosssection [7-11]. In 2004, these scientists found a reason to explain its, that was called solid state internal conversion [5]. Finally, in 2009, these authors mentioned a metal with its lattice structure and entered the lattice shape of the solid in their internal conversion calculations [12]. Their calculations were performed just for $D(p,\gamma)^3\text{He}$ reaction.

The aim of this work is modification Peter Kalman and Thomas Keszthelyi studies to the other fusion reactions such as $D(d,p)\text{T}$, $D(d,\gamma)^4\text{He}$, $T(d,n)^4\text{He}$ of fusion cross section with regarding the lattice effect in solid state internal conversion (LEISSIC). For reaching to this goal this article are divided into five general steps. In the first step, we explain how deuteriums were solved in palladium lattice as a sublattice. In the second step, the cross section of ordinary state for particular reactions is computed. In the third step, the cross section for three selected reactions in addition to $D(p,\gamma)^3\text{He}$: $D(d,p)\text{T}$, $D(d,\gamma)^4\text{He}$, $T(d,n)^4\text{He}$ are calculated. In the fourth step our obtained results of second and third steps are compared. In the five steps, the solid state internal conversion coefficient will be calculated in the presence of lattice effect. Finally, our obtained results are summarized.

2. Method of locating deuterium inside Palladium when deuterium inserted into palladium crystal [13, 14]

Pons and Fleischmann used cathodes including bulk materials (like plates, rods, wires) in their experiments, but here we use 'atomic cluster' or nanoparticles. Here, there is a Double Structure cathode ("DS"-cathode) (figure 1.) [15]. DS cathode is made by two parts which is divided into internal cathode (black **pd**) and external cathode (**pd plate**). Palladium is a transition metal and black palladium is a very fine powder in the form of nanoparticles which is called atomic cluster and it is kept in a vacuum cavity inside palladium **plate**. In comparison to bulk cathode, DS cathode provides the following applications:

- More than 100 percent** of deuteriums immediately are absorbed in internal volume of all black Pd particles because of "diffusion effect" and "atomic cluster effect".
- The purity degree of deuterium in DS cathode is so high due to "filtering effect" of palladium rod.
- Because of the enhancement pressure of deuteriums, the palladium rod obeys from Sieverts law.

In order to carry on the electrolysis in the electrolyte of D_2O/H_2O , this ultra-vacuum cavity inside the Pd rod could easily accommodate highly pure D_2/H_2 gas at over 1000 atm, which is due to following Sievert law.

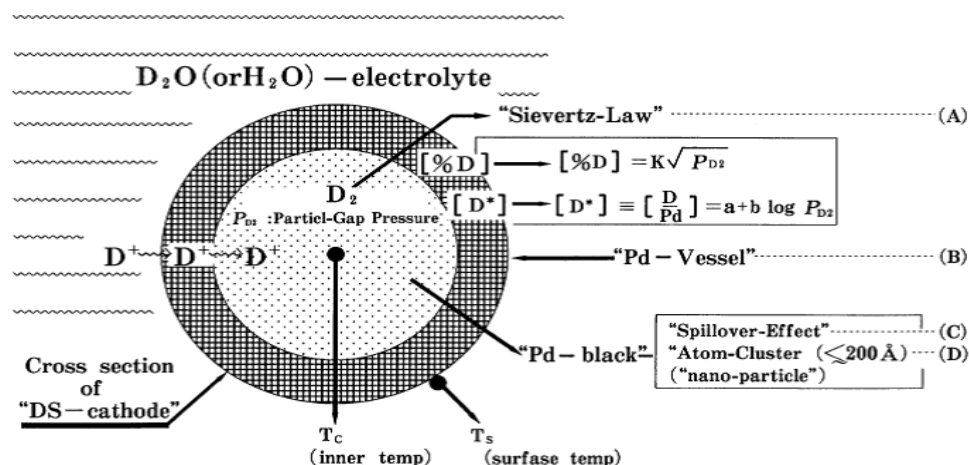


Figure1: The concept of DS cathode (double structure cathode). (A) High pressure of D₂ gas happens easily inside DS cathode because of Sievert law. (B) The purity of deuterium in a DS cathode is too high because a palladium rod acts like a filter. (C) because of the diffusion effect, deuterium immediately distributes on the surface of all black palladium particles uniformly and with a very high density. (D) Nano scale black palladium absorbes many deuteriums with more than 100 percent volume owing to atomic cluster effect.

FCC structure of solid palladium and octahedral structure which is sites of deuterium sublattice are respectively shown in Figs 2 and 3. Each palladium unit cell has four palladium atoms distinctively. Thus, each palladium atom in the corners belongs to eight different unit cells in its neighborhood. Since, we have eight atoms in the corners; therefore, each unit cell receives one palladium atom. Every atom is placed on each sides of cube which is contributed between two neighboring unit cells and because there are six atoms on the sides then each unit cell contains three atoms. One of the palladium unit cells has twenty one sites for deuteriums that are located in the sublattice. These twenty one sites are included octahedral, tetrahedral containers and can occupy by twelve deuteriums[13].

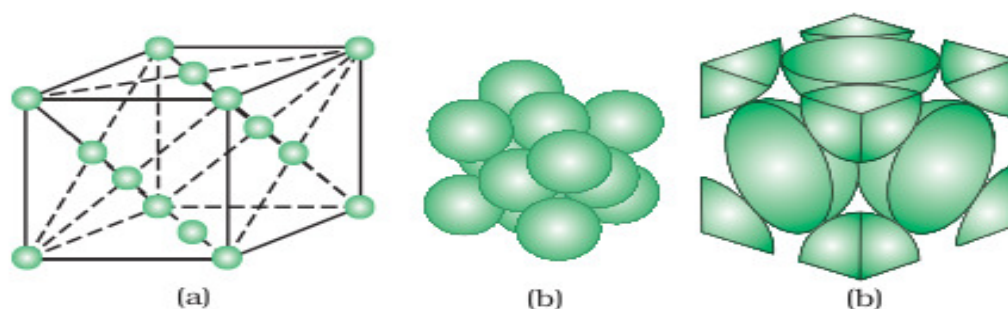
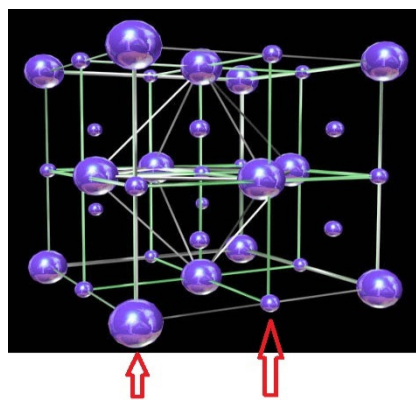


Figure 2: A face-centered cubic palladium unit cell (a). Open structure (b) space filling structure (c) actual portions of atoms belonging to one palladium unit cell.



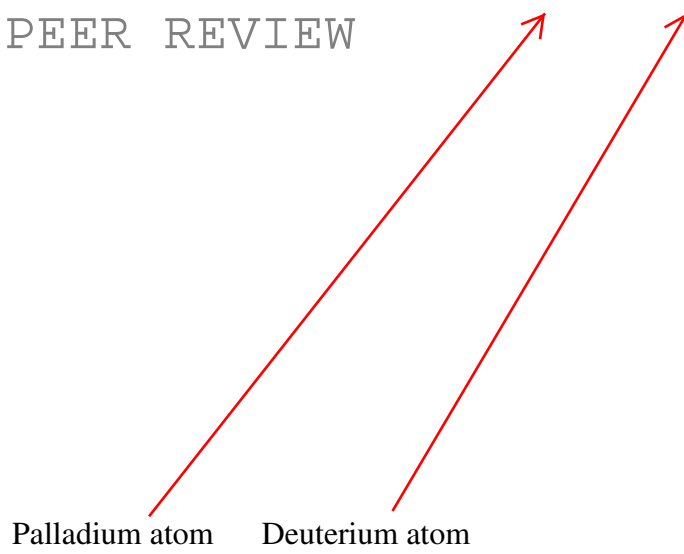


Figure 3: the schematic of deuterium atom as a sublattice in palladium unit cell, where big ball and small ball show palladium site in FCC lattice and deuterium atom in octahedral site in the sublattice, respectively.

Among these twenty one sites, eight of them are tetrahedral containers and the rest are octahedral containers. In each tetrahedral container only one deuterium can exist which is not stable while every octahedral container can accommodate from 1 to 4 deuteriums. As a result, one unit cell of palladium includes high density of deuterium. This deuterium slice in the palladium unit cell is called pycnodeuterium (Figure 4), “pycno” means high density. Because of high density of deuterium in every palladium unit cell, each unit cell is known as a small cold fusion reactor [14].

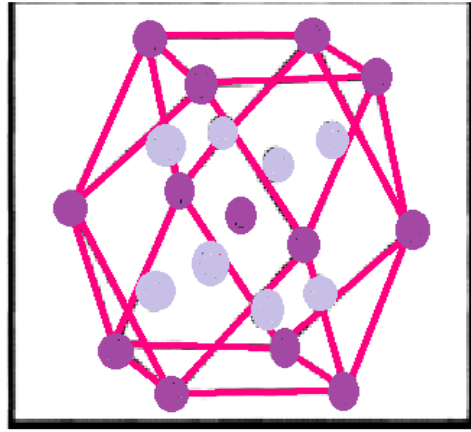


Figure 4: the schematic of the pycnodeuterium slice formed in palladium unit cell.



Tetrahedral container.



Octahedral container.

3. The scrutiny on the fusion cross section of ordinary state

Whenever the expression “Ordinary State” is appeared means that in determination of cross section, LEISSIC is not considered. Using the extrapolation, the fusion cross section, $\sigma(E)$ of an induced-charged-particle nuclear reaction in the astrophysical energies is given by [7],

$$\sigma(E) = S(E)E^{-1} \exp(-2\pi\eta(E)) \quad (1)$$

Where, $\eta(E)$ and $S(E)$ are the Sommerfeld parameter and the astrophysical S-factor, respectively. It is assumed that the Coulomb potential of the target nucleus and projectile is the result of bare nuclei.

The numerical values of $S(0)$ were calculated completely in the ref 16. Here, our investigation are performed on the low energy (5-30 eV), the values of $S(0)$ for each reaction is assumed to be constant which are listed in table 1 for different fusion reactions.

Table 1: the numerical values of astrophysical S-factor for different fusion reactions in ordinary state in low energy

Reactions				
Astrophysical factor	$D(p,\gamma)^3\text{He}$	$D(d,p)\text{T}$	$D(d,\gamma)^4\text{He}$	$T(d,n)^4\text{He}$
$S(0)$ MeV barn	0.2×10^{-6}	0.056	0.054	10

The cross section for ordinary state in terms of incoming particle energy are represented in Fig.5 using Eq.1.

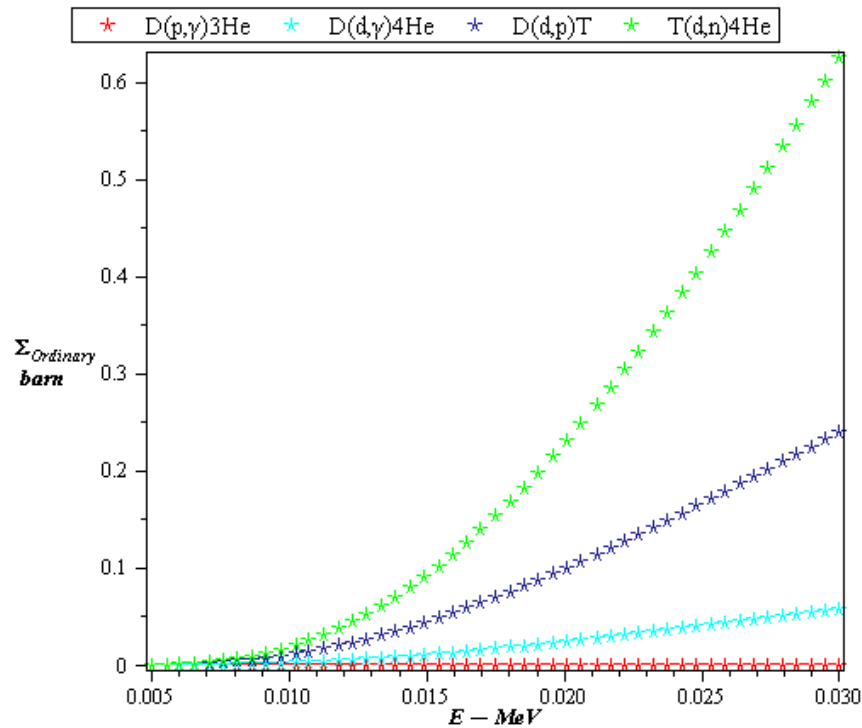


Figure 5: The two dimensional variation of fusion cross section in terms of incoming energy for selected reactions in ordinary state. Each color shows one kind of reaction. Green, dark blue, light blue, and red represent $T(d,n)^4\text{He}$, $D(d,p)\text{T}$, $D(d,\gamma)^4\text{He}$ and $D(p,\gamma)^3\text{He}$ respectively. From this figure we observed that by increasing E , fusion cross section of ordinary state (Σ_{ordinary}) increases too.

4. Determination of fusion cross section with LEISSIC

The electron clouds surrounding the interacting nuclides act as a screening potential and withreducing Coulomb barrier whichis essential for performing fusion reaction. This mechanism

which discussed in section 3 increases the cross section in comparison with the previous state (Ordinary cross section) [3]. The internal conversion(IC) might take place in solid environment between fusible nuclides and each charged particle in the crystal. IC can involve a transition between internal layers of atoms. The particle that transit can be different. In solid state internal conversion (SSIC) there are both electron and deuterium transition [5]. Therefore, enhancement of cross section in the crystal can be due to IC in extra channels (such as electron and deuterium channels).

4.1. Formulation and importing LEISSIC

Since particles in the crystal are placed in specific sites, we can estimate fusion cross section (FCS) reactions using Block theorem for describing initial and final states of this system (palladium environment). In all formulas subscripts 1, 2 and 3 are respectively pointed at incoming, sublattice and host particles. Also, the state of particles in the lattice is determined by Block function [17]

$$\varphi_{k_3,i}(r_3) = \frac{1}{\sqrt{N}} \sum_{l_s} e^{ik_3 \cdot l_s} a_3(r_3 - l_s - u_3(l_s)) \quad (2) \longrightarrow$$

where, r_3 , $k_{3,i}$ and a_3 are respectively introduced host-particle coordinate, a wave vector of the first Brillouin zone of the reciprocal lattice, and Wannier function. Here, Pd (palladium), d (deuteron) and e (electron) are considered as host particles. Lattice site and the displacement of the atom located at lattice site are symbols to represent l_s and $u_3(l_s)$. Here N is the number of lattice point. The sublattice particle also is described by Block function (Eq 3). Lattice contains N_2 fusible particles, for palladium system it is assumed that $N_2 = N$.

$$\varphi_{k_2,i}(r_2) = \frac{1}{\sqrt{N_2}} \sum_{l_s} e^{ik_2 \cdot l_s} a_2(r_2 - l_s - u_2(l_s)) \quad (3) \longrightarrow$$

Here, a_2 and a_3 are Wannier functions for sublattice and host particles respectively that are determined by equation 4 \longleftarrow

$$a_j(x) = \left(\frac{\beta_j^2}{\pi} \right)^{3/4} e^{-\frac{\beta_j^2}{2} x^2} (x = r_2 - l_s), j = 2, 3 \quad (4)$$

In the above formula, $\beta_j = \sqrt{m_j \omega_j / \hbar}$ [18]. The initial state Ψ_i for the three particles that participate in solid state assisted fusion reaction is described by,

$$\Psi_i = \varphi_{k_2,i}(r_2) \varphi_{k_3,i}(r_3) \varphi_1(r_1 - r_2) \quad (5) \longrightarrow$$

where, $\varphi_1(r_1 - r_2)$ is the Coulomb wave function corresponding to the state of a sublattice and incoming particle. The Coulomb wave function is φ_1 \longleftarrow

$$\varphi_1(r_1 - r_2) = e^{ik_1 \cdot (r_1 - r_2)} \frac{f(k_1, r_1 - r_2)}{\sqrt{V}} \quad (6)$$

V is the volume of normalization, k_1 is the wave vector, r_1 is the coordinate of incoming particle, and f function is defined as the following [7]:

$f(k_1, x) = e^{-\pi\eta/2} \Gamma(1 + i\eta) {}_1F_1(-i\eta, 1; i[k_1 x - \mathbf{k}_1 \cdot \mathbf{x}])$ (7) ${}_1F_1$ is the confluent hyper geometric function [19]. η is determined by using the eq. 8 and 9 [16].

$$\eta = 0.1575 z_1 z_2 \left(\frac{A}{E}\right)^{1/2} \quad (8)$$

$$A = \frac{A_1 A_2}{A_1 + A_2} (amu) \quad (9)$$

where z_1 and z_2 are the charge number of particles 1 and 2 and E is the energy of incoming particle. A_1 and A_2 are the mass of incident and sublattice particles that are measured in amu unit. The final state of this three-body system is,

$$\Psi_f = \psi_f(r_1, r_2) \varphi_f(r_3) F_{cb}(z_3, z_{12}, v_{3,12}) \quad (10)$$

Where φ_f is a plane wave of wave vector k_3 that is corresponded to an outgoing particle 3.

$$\varphi_f(r_3) = \frac{1}{\sqrt{V}} e^{ik_3 \cdot r_3} \quad (11)$$

ψ_f stands for the outgoing fusion product leaving a deuteron lattice point vacancy that the relative coordinate and the center of mass coordinate of the particles of the rest masses m_1 and m_2 are given by: $r = r_1 - r_2$ and $R = m_1 r_1 + m_2 r_2 / m$ respectively, then we have

$$\psi_f(r, R) = \frac{1}{\sqrt{V}} e^{iK \cdot R} \chi(r) \quad (12)$$

where K and $\chi(r)$ are the wave vector of fusion product and a nuclear wave function, respectively.

$$\chi(r) = \left(\frac{\lambda^2}{\pi}\right)^{3/4} e^{-\lambda^2 r^2 / 2} \quad (13)$$

The Coulomb interaction between host particle and the product of the incident and sublattice reaction are represented as following by using the Fermi correction;

$$F_{cb} = \sqrt{2\pi\xi} \frac{e^{-\pi\xi}}{\sqrt{1 - e^{-2\pi\xi}}} \quad (14)$$

Here, $\xi = z_3 z_{12} \alpha_f \sqrt{\mu c^2 / 2Q}$ and also α_f is known as the fine structure constant. μ is the reduced mass;

$$\mu = \frac{(m_1 + m_2)m_3}{m_1 + m_2 + m_3} \quad (15)$$

the element of s-matrix that is used for determining of the cross section of the different fusion reaction is known as,

$$S_{fi} = \frac{2\pi}{i\hbar} \iiint \Psi_f^* \frac{z_1 z_3 e^2}{|r_1 - r_3|} \Psi_i d^3 r_1 d^3 r_2 d^3 r_3 \delta(E/\hbar) \quad (16)$$

with a little simplification on this integral and using the Hartree-Fok approximation for Coulomb interaction part of integral, we have

$$\frac{z_1 z_3 e^2}{|r_1 - r_3|} = \frac{z_1 z_3 e^2}{2\pi^2} \int d^3 q \frac{1}{q^2} e^{iq \cdot (r_1 - r_2)} \quad (17)$$

Putting the Fourier transform of Eq.13 in Eq.16, and applying the approximation 17 and comparing it with $\langle \sigma v \rangle$ formula, the cross section of fusion reaction between host and target fusible particles is obtained as the following,

$$\sigma_2 = C_0 \frac{\exp(-2\pi\eta)}{E} \quad (18)$$

E is the energy of incoming particle and C_0 is determined by,

$$C_0 = |F_{cb}|^2 A_0 k_\mu \left(\frac{\beta_2}{K_Q} \right)^3 \langle |\tilde{\chi}|_{K=K_Q}^2 \rangle_{\Omega_K} \quad (19)$$

with Ω_K denoting the solid angle in the K space, $\beta_2 = \sqrt{m_d \omega / \hbar}$, $A_0 = 128 \alpha_f^3 z_1^3 z_3^2 z_2 m_1 c^2 \sqrt{\pi}$, $K_Q = \sqrt{2\mu c^2 Q} / (\hbar c)$, Q is the energy of the reaction, and $k_\mu = \mu c / \hbar$. The average of nuclear wave function is defined by,

$$\langle |\tilde{\chi}|_{K=K_Q}^2 \rangle_{\Omega_K} = \left| \tilde{\chi} \left(\frac{m_2}{m} K \right) \right|^2 = \frac{8\pi^{3/2}}{\lambda^3} e^{-\frac{4K^2}{9\lambda^2}} \quad (20)$$

m_n , nucleons mass, ω_n angular frequency of binding energy are calculated for each reaction separately

$$\lambda = \frac{\sqrt{m_n \omega_n}}{\hbar} \quad (21)$$

$$m_n = m_i + m_{He}, i = d \text{ or } t \quad (22)$$

$$\omega_n = \frac{\text{binding energy of He (MeV)}}{\hbar} \quad (23) \quad \longrightarrow$$

The numerical values of m_n , ω_n , λ and binding energy of He are calculated and listed in Table.4. Here, C_0 is computed for one d or one Pd. In order to compare C_0 with astrophysical factor (S(0)) in ordinary state, the density of these particles must be accounted. So, we use Eq.24,

$$NC_0 = A \Delta R_h C_1 \quad (24)$$

such that, N is,

$$N(Pd) = V_{eff} / v_{cell} \quad (25)$$

Where $v_{cell} = d^3 / 4$, $V_{eff} = A \Delta R_h$ and $d = 3.89 \times 10^{-8} \text{ cm}$ is the lattice constant

$$N(d) = u V_{eff} / v_{cell} \quad (26)$$

In Eq.23, u is the ratio of deuteron to palladium number density. For electron $u = 10$ which is the number of electron valence in palladium. C_0 contains all the properties of the lattice. For comparing the fusion cross section with and without LEISSIC we have to determine the macroscopic cross section:

$$\Sigma = N \sigma_2 \quad (27)$$

5. Results of numerical calculations for each reaction

Tables 2 and 3 can aid in plotting the cross section for all reactions and comparing with the ordinary state. The hypotheses of host, sublattice and incoming particles are expressed for all reactions in this way: the host particles are Pd, d, e for Palladium. The sublattice is deuterium for all reactions. The incoming particles are proton (p) in $D(p,\gamma)^3\text{He}$, deuterium (d) in $D(d,p)\text{T}$ and $D(d,\gamma)^4\text{He}$ and tritium (t) in $T(d,n)^4\text{He}$. Our calculations for obtaining the cross section for all three kind of host particles are accomplished by using equations: 14, 15, 19, 20 and 24 and our obtained results are given in tables 2 and 3.

Table 2: Our numerical calculations of necessary quantities for obtaining C_0 for all chosen reactions

Type of Reactions	host particles	A_0 (MeV)	$\mu(\text{gr})$	$K_Q(\text{cm}^{-1})$	$ \tilde{\chi} _{\vec{k}=\vec{K}_Q}^2$ (cm^3)	ξ
$D(p,\gamma)^3\text{He}$	Pd	175	5.013×10^{-24}	8.91×10^{12}	3.95×10^{-38}	10.755
	d	0.0827	2.005×10^{-24}	5.64×10^{12}	5.13×10^{-38}	0.1477
	e	0.0103	-----	2.78×10^{11}	6.11×10^{-38}	-560382
$D(d,p)\text{T}$	pd	349	6.686×10^{-24}	8.82×10^{12}	3.15×10^{-38}	14.462
	d	0.165	2.229×10^{-24}	5.09×10^{12}	3.97×10^{-38}	0.181
	e	0.021	-----	2.05×10^{11}	4.45×10^{-38}	-0.0011
$D(d,\gamma)^4\text{He}$	Pd	349	6.686×10^{-24}	7.93×10^{12}	3.69×10^{-38}	16.075
	d	0.165	2.229×10^{-24}	4.58×10^{12}	4.51×10^{-38}	0.202
	e	0.021	-----	1.65×10^{11}	4.98×10^{-38}	-0.0022
$T(d,n)^4\text{He}$	Pd	524	8.35×10^{-24}	2.05×10^{13}	2.89×10^{-39}	5.863
	d	0.248	2.387×10^{-24}	1.10×10^{13}	4.24×10^{-39}	0.09
	e	0.031	-----	8.90×10^{11}	4.30×10^{-38}	-4.228

From the results of Table 2 and Eqs. 19 and 24 for different reactions and host particle, we can calculate the required parameters such as C_0 and C_1 which are important for estimating cross section of the fusion reactions.

cm , vertical letters

Table 3: our numerical calculation C_0 and C_1 for different host particle and different reactions

Type of Reactions	host particles	k_μ (cm^{-1})	$ F_{cb} ^2$	C_0 (MeV b)	C_1 (MeV b)
$D(p,\gamma)^3He$	Pd	1.42×10^{14}	3.14×10^{-28}	4.92×10^{-38}	3.36×10^{-24}
	d	0.57×10^{14}	0.61	2.30×10^{-13}	$u \times 15.6$
	e	-----	1	9.10×10^{-13}	6.18×10^2
$D(d,p)T$	Pd	1.90×10^{14}	3.27×10^{-38}	1.11×10^{-47}	7.53×10^{-34}
	d	0.63×10^{14}	0.5371	1.88×10^{-13}	$u \times 12.78$
	e	-----	1	2.48×10^{-12}	1.687×10^3
$D(d,\gamma)^4He$	Pd	1.90×10^{14}	7.02×10^{-41}	3.83×10^{-50}	0.26×10^{-35}
	d	0.63×10^{14}	0.4964	2.70×10^{-13}	$u \times 18.35$
	e	-----	1	4.31×10^{-36}	2.93×10^{-21}
$T(d,n)^4He$	Pd	2.37×10^{14}	4.44×10^{-15}	2.05×10^{-25}	1.39×10^{-12}
	d	0.68×10^{14}	0.7438	4.45×10^{-15}	$u \times 0.3024$
	e	-----	1	1.87×10^{-13}	127.1

Since each palladium unit cell has 4 Pd atoms purely and since we suppose that the number of host and sublattice particles are equal, then we have

$$N_{Pd} = \frac{1}{4} \times 4.22 \times 10^{22} \quad (28)$$

The other quantities such as λ , β_2 and Q which is mentioned before are calculated and numerical results are summarized in Table 4.

Table 4: Required quantities which are calculated for determination of different fusion

Type of Reactions	λ (cm^{-1})	β_2 (cm^{-1})	Q (MeV)	Binding Energy (MeV)
$D(p,\gamma)^3He$	9×10^{12}	4.81×10^{14}	5.49	7.718
$D(d,p)T$	10×10^{12}	4.81×10^{14}	4.04	8.482
$D(d,\gamma)^4He$	9.63×10^{12}	4.81×10^{14}	3.27	28.3
$T(d,n)^4He$	21.8×10^{12}	4.81×10^{14}	17.59	28.3

6. Microscopic and macroscopic fusion Cross Section

The fusion cross section of each mentioned reactions is divided into three parts because we have three host particles (Pd,d,e). In addition there are two kinds of fusion cross

section:Microscopic (mic) (Figure 6, 7) and macroscopic (mac) (Figure 8, 9) cross sections which are plotted for different reactions by considering different host particles using Eqs.18 and 27 and the values of C_0 in table 3, respectively. The macroscopic cross section is compared with ordinary state (Figs. 10 to 13). We use $\sigma_i a(x, y)b$ and $\Sigma_i a(x, y)b$ to introduce the microscopic and macroscopic fusion cross section respectively, for each reaction with different host particle where, $i= Pd, d, e$ and $a(x, y)b$ is one of the nuclear reaction. For example, $\sigma_e T(d, n) {}^4He$ is the fusion cross section(FCS)means that electron host particle for $T(d, n) {}^4He$.

For showing mic and mac FCS schematics more clearly, all graphs are divided into aseven maximum (Figs. 6 and 8) and five minimum (Figs. 7 and 9) diagrams. In Figs. 6 to 9, “Green” color indicates $T(d, n) {}^4He$ reaction, “red”, “dark blue” and “dark pink” indicates $D(p, \gamma) {}^3He$, $D(d, p)T$ and $D(d, \gamma) {}^4He$ respectively. We can also realize the kind of host particle by noticing the style of the graph e.g. “Dash” shows Pd, “Long Dash” electron and “Dash Dot” for d.

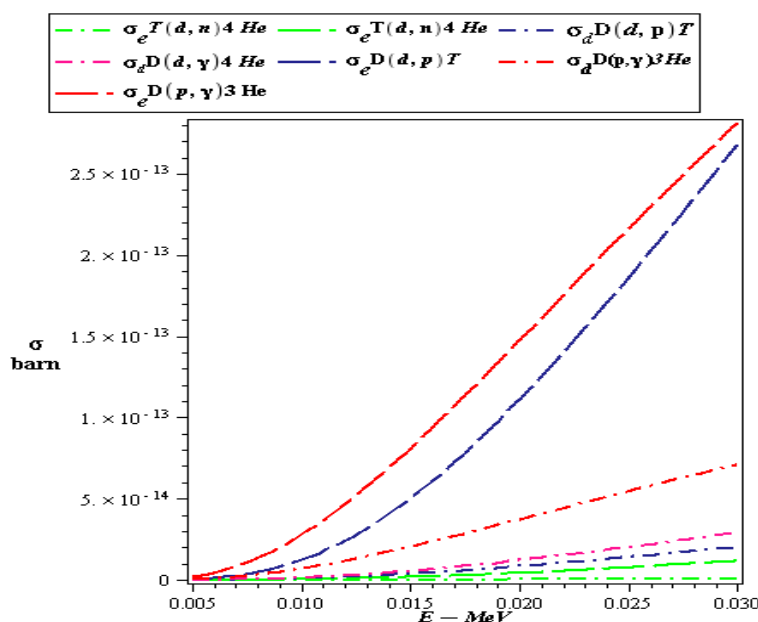


Figure 6: The two dimensional seven maximums modes microscopic cross section as a function of the incoming particle energy for different host particles and different reactions. **the** maximum cross sections belong to electron and deuteron host particles and the best reactions are $D(p, \gamma) {}^3He$ and $D(d, p)T$.

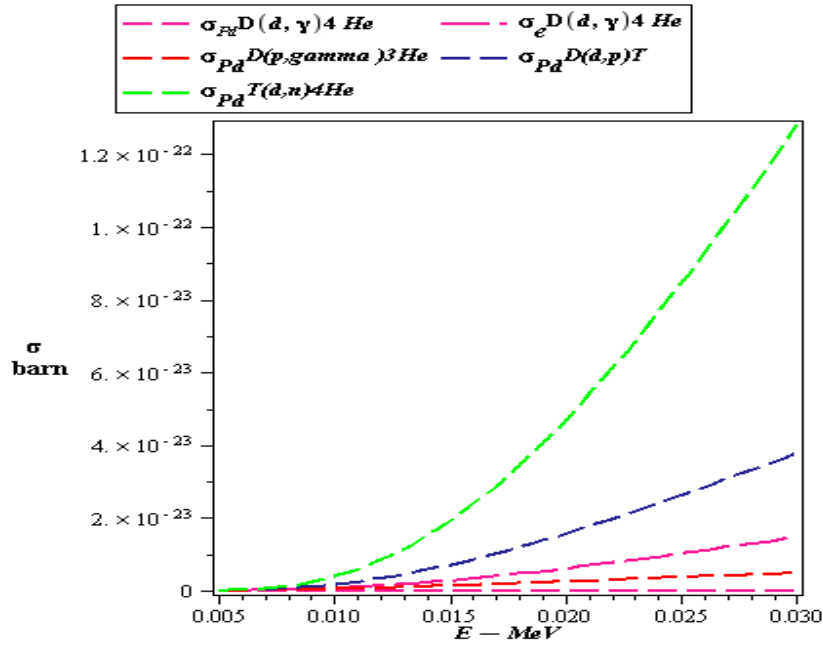


Figure 7: The five minimum microscopic crosssection as a function of the incoming for different host particles and different reactions. In this graph the maximum cross sections belong to palladium host particle for $T(d,n)^4\text{He}$ and $D(d,p)T$.

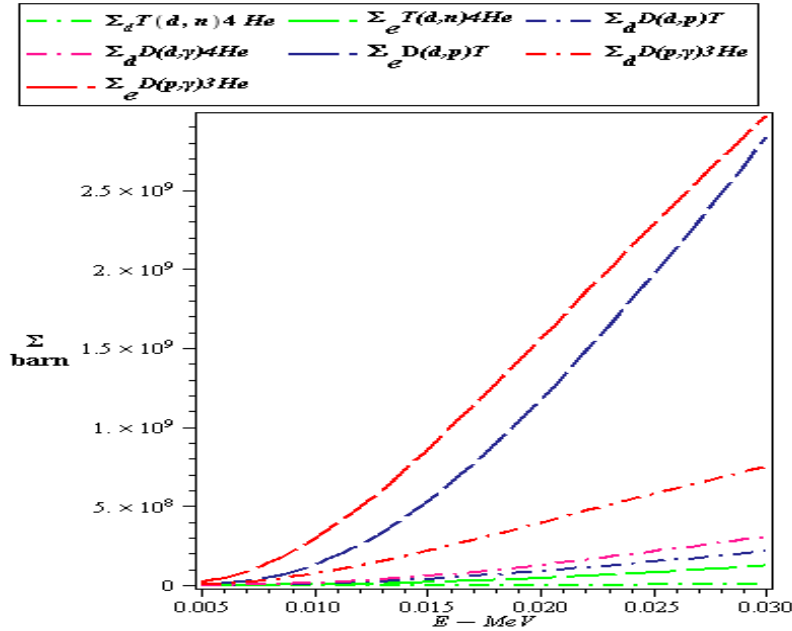


Figure 8: The two dimensional seven maximums macroscopic cross section as a function of the incoming particle energy for different host particles and different reactions. The maximum cross sections belong to electron and deuteron host particles. The best reactions are $D(p,\gamma)^3\text{He}$ and $D(d,p)T$.

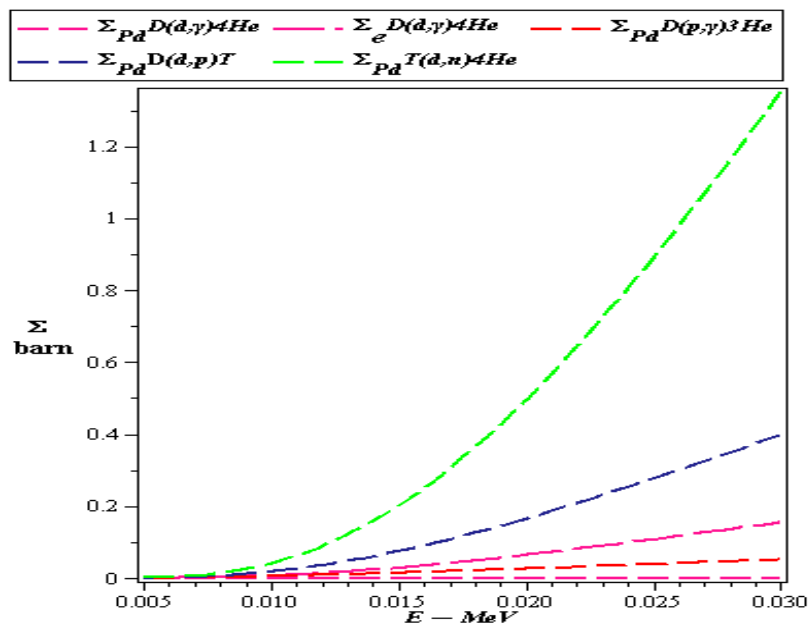


Figure 9: The two dimensional five minimum macroscopic cross sections as a function of the incoming particle energy for different host particles and different reactions. The maximum cross section belongs to palladium host particle for $T(d,n)^4\text{He}$ and $D(d,p)T$.

Figs. 6 to 9 emphasize that the electron and deuteron host particles represent the maximum cross sections. Among of all reactions $D(d,p)T$ is the best reaction because it has maximum cross section but the numerical difference between $D(d,p)T$ and $T(d,n)^4\text{He}$ is low.

Now for comparison the ordinary and macroscopic FCS with regarding LEISSIC, we plotted Figs. 10,11,12 and 13. In this case, green, dark blue and red colors indicate the cross section of electron, deuteron and Pd as a host particles selection respectively. The light blue implies ordinary FCS.

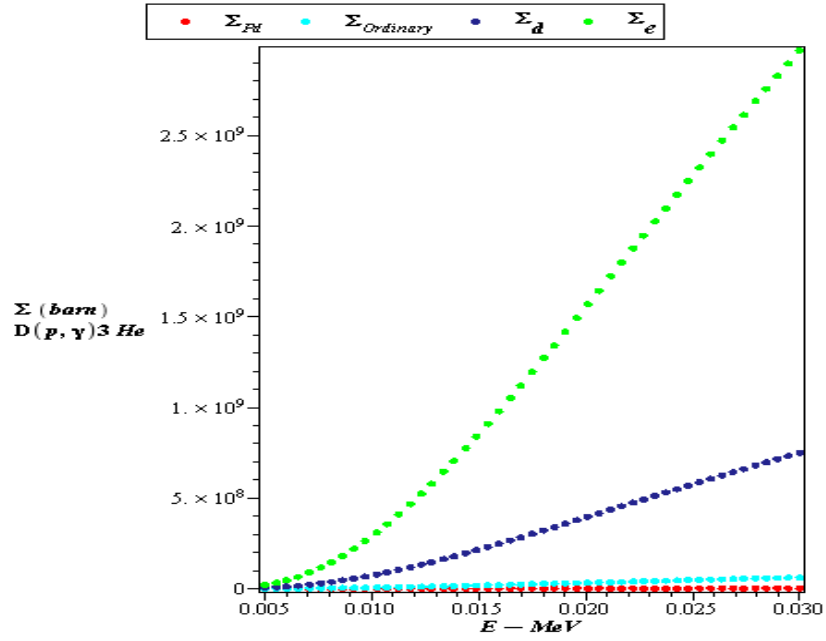


Figure 10: The macroscopic cross section for $D(p, \gamma)^3\text{He}$ reaction with regarding different host particles and ordinary state in terms of incoming particle energy. It shows the comparison of the cross section of LEISSIC with ordinary cross section for $D(p, \gamma)^3\text{He}$ reaction. The only graph that is lower than ordinary state is the palladium graph.

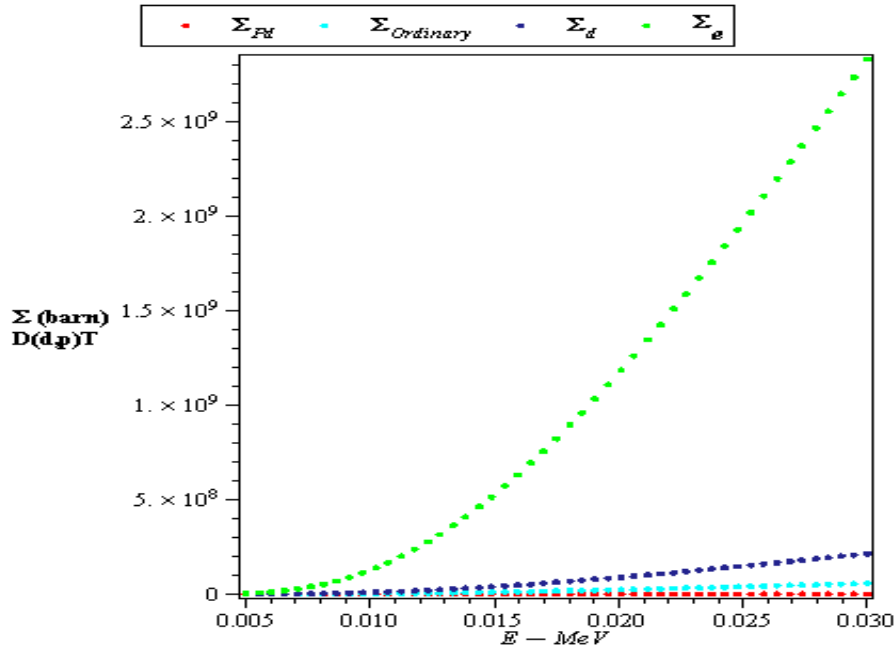


Figure 11: The macroscopic cross section for $D(d, p)T$ reaction with regarding different host particles and ordinary state in terms of incoming particle energy. It shows the comparison of the cross section of LEISSIC with ordinary cross section for $D(d, p)T$ reaction. The only graph that is lower than ordinary state is the palladium graph.

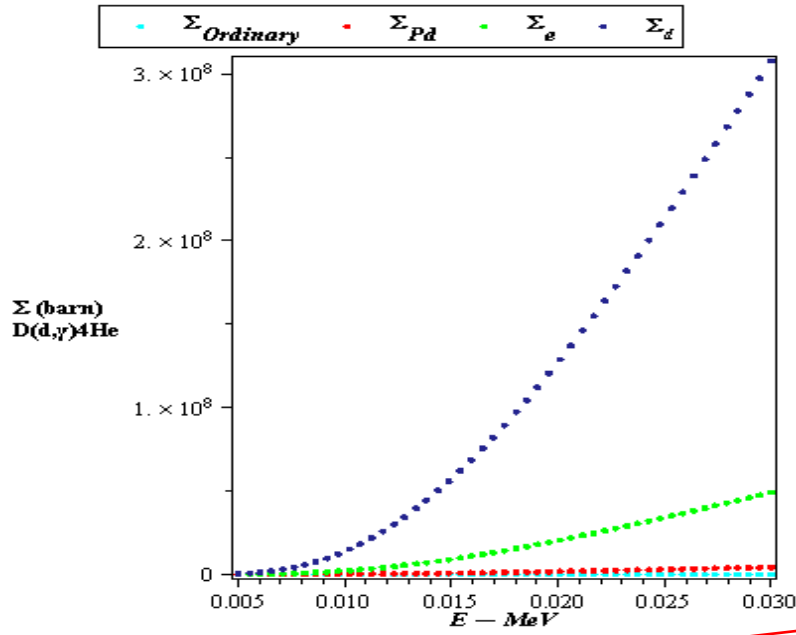


Figure 12: The macroscopic cross section for $D(d,\gamma)^4\text{He}$ reaction with regarding different host particles and ordinary state in terms of incoming particle energy. It shows the comparison of the cross section of LEISSIC with ordinary cross section for $D(d,\gamma)^4\text{He}$ reaction. The only graph that is lower than ordinary state is the palladium graph

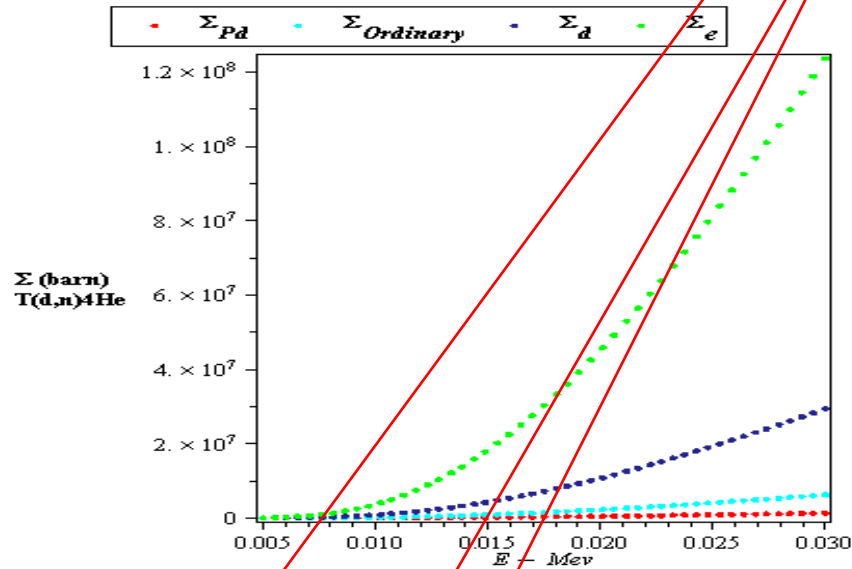


Figure 13: The macroscopic cross section for $T(d,n)^4\text{He}$ reaction with regarding different host particles and ordinary state in terms of incoming particle energy. It shows the comparison of the cross section of LEISSIC with ordinary cross section for $T(d,n)^4\text{He}$ reaction. The only graph that is lower than ordinary state is the palladium graph

For comparing different host particle cross section such as $D(p,\gamma)^3\text{He}$, $D(d,p)\text{T}$ and $T(d,n)^4\text{He}$, we have $\Sigma_e > \Sigma_d > \Sigma_{pd}$ but just for $D(d,\gamma)^4\text{He}$ $\Sigma_d > \Sigma_e > \Sigma_{pd}$. Also, from comparing different host particle cross section with ordinary cross section, we have $\Sigma_e > \Sigma_d > \Sigma_{\text{ordinary}} > \Sigma_{pd}$ for all kind of reactions except $D(d,\gamma)^4\text{He}$. By comparing LEISSIC and ordinary cross sections, we

distinguish that the ordinary cross section is minimum. As results show, graphs verify the theory that expresses “there is a magnificent enhancement in cross section when we consider lattice effect in solid state internal conversion in our calculations”.

7. Calculations of the solid state internal conversion coefficient for different fusion reactions in Palladium crystal environment

With regarding to definition that exists in Ref.12, we can write $v_{eff} = A\Delta R_h$, where A is the cross section of the beam, ΔR_h is the “differential” range, which is, the distance within the energy of the incoming particle can be considered unchanged. The $\Delta R_h \ll R_h$ condition helps in an order of magnitude estimate of ΔR_h , where R_h is the stopping range of a proton which is about $8 \times 10^{-2} \mu m$ at $E = 0.01 \text{ MeV}$ in Pd [20]. The quantities A and R_h were measured in mm^2 and $10^{-3} \mu m$ units. The solid state internal conversion coefficient is introduced as,

$$\alpha_{SSIC} = A\Delta R_h C_1 / S(0) \quad (29)$$

By using the amounts exist in tables 1, 3 and replacing them inside Eq.29 the solid state internal conversion coefficient for different reactions can be found. This coefficient represents the internal conversion rate in different reactions. The results of our calculations are summarized in table 5.

Table 5: The values of solid state internal conversion coefficient in different reactions for e, 4d and d channels

Reactions	$\alpha_{SSIC,d} A\Delta R_h$	$\alpha_{SSIC,e,4d} A\Delta R_h$
D(p, γ) ^3He	$u \times 7.8 \times 10^5$	3.1×10^9
D(d,p)T	$u \times 3.03 \times 10^4$	3.2×10^6
D(d, γ) ^4He	$u \times 3.398 \times 10^2$	5.42×10^{-20}
T(d,n) ^4He	$u \times 0.03$	12.7

We obviously see from this table that solid state internal conversion more occurs in D(p, γ) ^3He and D(d,p)T reactions.

8. Conclusion

By reviewing all of our calculations, we understand that the lattice effect in solid state internal conversion cross section is more than ordinary state for each reaction. In previous experiments the complete reason for increasing cross section experimentally for these reactions are not explained but in this work by analyzing LEISSIC we can justify those observations theoretically. Our theoretical studies prove that the results of the experiments are given in below.

Whenever we consider the crystalline lattice in our calculations, since deuteriums and the other fusible particles are solved inside a lattice as a sublattice, the required energy for locating these particles in a regular shape in the lattice reduces the Coulomb barrier more than

before and increases the probability of fusion reaction. Therefore, when fusion reactions happen in the crystalline solid state environment the effect of lattice in solid state internal conversion processes cannot be neglected.

From graphs and internal conversion mechanism, we understand that since the internal conversion rates of $D(p,\gamma)^3\text{He}$ and $D(d,p)\text{T}$ reactions are more than others, they are the best choices to study.

9. References

[1] US DOE 1989, p. 7

[2] "60 Minutes: Once Considered Junk Science, Cold Fusion Gets A Second Look By Researchers". CBS. 2009-04-17. <http://www.cbsnews.com/stories/2009/04/17/60minutes/main4952167.shtml>.

[3] www.wikipedia.com

[4] Taubes 1993, pp. 136–138.

[5] P. Kalman and T. Keszthelyi, Phys. Rev. C **69**, 031606(R) (2004).

[6] Biberian 2007.

[7] F. Raiola *et al.*, Eur. Phys. J. A **13**, 377(2002); Phys. Lett. **547**, 193 (2002).

[8] C. Bonomo *et al.*, Nucl. Phys. **A719**, 37c (2003).

[9] J. Kasagi *et al.*, J. Phys. Soc. Jpn. **71**, 2881 (2002).

[10] K. Czerski *et al.*, Eur. Phys. Lett. **54**, 449 (2001); Nucl. Instrum. Methods Phys. B **193**, 183 (2002).

[11] A. Huke, K. Czerski, and P. Heide, Nucl. Phys. **A719**, 279c (2003).

[12] P. Kalman and T. Keszthelyi, Phys. Rev. C **79**, 031602(R) (2009).

[13] Y. Arata and Y. C. Zhang: *Proc. Jpn Acad. B*, **78** (2002) 57.

[14] Y. Arata and Y. C. Zhang: *J. High Temp. Soc. Jpn.* **29** (Special Vol.) (2008), 1-44; ICCF10.

[15] Y. Arata and Y. C. Zhang: *Proc. Jpn. Acad. B*, **70** (1994) 106; **71** (1995) 304; *Jpn. J. Appl. Phys.*, **37** (1998) L1274; **38** (1999) L774.

[16] C. Angulo *et al.*, Nucl. Phys. **A656**, 3 (1999).

[17] J. M. Ziman, *Principles of the Theory of Solids* (Cambridge University Press, Cambridge, 1964), pp. 148-150.

[18] C. Cohen-Tannoudji, B. Diu, and F. Laloë, Quantum Mechanics, Vol. 1 (Wiley, New York [English version]/Hermann, Paris, 1977).

[19] K. Alder *et al.*, Rev. Mod. Phys. **28**, 432 (1956).

[20] R. B. Firestone and V. S. Shirley, Tables of Isotopes, 8th ed. (wiley, New York, 1996).